Mechanism for *p*-type conduction in polycrystalline indium oxide films

Jolanta Stankiewicz,[1,*] María Pilar Lozano,[2] and Francisco Villuendas[3]
[1]*Instituto de Ciencia de Materiales de Aragón and Departamento de Física de la Materia Condensada, CSIC–Universidad de Zaragoza, 50009 Zaragoza, Spain*
[2]*Instituto Tecnológico de la Construcción, 46980 Paterna–Valencia, Spain*
[3]*Departamento de Física Aplicada, Universidad de Zaragoza, 50009 Zaragoza, Spain*
(Received 25 September 2011; revised manuscript received 26 December 2011; published 14 March 2012)

We report results of ac impedance measurements which we have obtained from intrinsic indium oxide films under UV irradiation and in darkness. We find two distinct contributions to the ac conductivity. One of them is brought about by grain boundaries, and the other one by inversion layers, which are on grain surfaces. In addition, we have found that photocurrents relax extremely slowly in these films. All of this fits consistently within a model in which mobile holes in inversion layers are responsible for recently reported *p*-type dc conductivity.

DOI: 10.1103/PhysRevB.85.125306 PACS number(s): 73.50.Pz, 73.61.Le, 73.20.Hb

I. INTRODUCTION

Indium oxide (IO) belongs to the family of transparent conducting oxides (TCO) which are used in a wide variety of modern technological applications. Such films are highly transparent in the visible wavelength range and show high electrical conductivity. They are used as low emissivity windows, gas sensors, transparent electrodes in flat panel displays, solar cells, and touch panels, among others.[1–5] Their usefulness is unfortunately hindered by difficulties in doping them into *p* type, which would render electronics all-transparent. The discovery that transparent $CuAlO_2$ thin films show appreciable room-temperature *p*-type conductivity has been an important advance in this direction.[6] Since then several *p*-type TCO, including technologically important ZnO, have been obtained.[7,8] As other transparent conducting oxides, IO shows many interesting physical attributes, and though it has been extensively studied, some of its fundamental properties are only just emerging. A recent impressive improvement in material quality has enabled researchers to establish the nature of the IO band gap.[9] However, the origin of a rather high free-electron concentration in as-grown thin films (between 10^{18} and 10^{20} cm^{-3}), remains a subject of intense debate. First-principles orbital molecular calculations show it most likely follows from the presence of interstitial indium and oxygen vacancies.[10] However, calculations which make use of density functional theory find that both interstitial and substitutional hydrogen act as shallow donors in indium oxide.[11] They would likely be responsible for IO's high conductivity, which is as suggested by muon spin rotation and relaxation experiments.[12] Existing defect models are inconclusive about the origin of conductivity in IO, but it is clear that native defects are relevant as donors and acceptors in transparent oxides.[13]

Indium oxide, which crystallizes in a cubic bixbyite structure, is a direct band-gap semiconductor. Close to stoichiometric composition, IO has low free-carrier concentration and high resistivity ($\rho \sim 10^8\ \Omega\,cm$). Recently, we have found that In_2O_3 thin films deposited by sputtering under O_2-rich conditions show *p*-type conduction, as confirmed by the sign of the Seebeck coefficient, Hall-effect measurements, and rectifying behavior of *p*-*n* homojunctions we have fabricated on these films.[14] This result is somewhat surprising since the formation energy of *p*-type defects in IO (such as indium vacancies or oxygen interstitials) is rather high.[15,16]

In order to cast some light on the physical mechanism underlying electronic transport in *p*-type films, we have performed a careful structural characterization on these films, in addition to ac impedance measurements under various conditions, including UV irradiation. The combined use of impedance spectroscopy (IS) and electron microscopy is a powerful means of characterizing materials.[17] These techniques allow one to obtain conductivity for different phases and, in certain cases, to derive microstructural information that is not accessible otherwise. Our experimental results can be consistently accounted for by a model we propose in which dc conduction in polycrystalline IO films grown under O_2-rich conditions takes place mainly in *p*-type inversion channels on the surface of crystalline grains (while the bulk of grains remains *n* type).

II. EXPERIMENT

We have grown IO thin films by dc magnetron sputtering from a ceramic IO target in a O_2/Ar atmosphere in a vacuum system with a base pressure of $\sim 4 \times 10^{-6}$ Torr. Fused-quartz substrates were kept at a constant temperature of 350 C. The total pressure during deposition was fixed at 1.1×10^{-3} Torr. Film thickness ranged from 50 to 500 nm. The structural characterization of the films was done using x-ray diffraction (XRD), scanning and transmission electron microscopy (SEM, TEM), and atomic force microscopy (AFM). Depth profiling was performed with x-ray photoelectron spectroscopy (XPS) in order to study oxygen spectra. ac impedance measurements were carried out with a precision impedance analyzer in the frequency range from 40 Hz up to 50 MHz. Several IO films, grown under various O_2 partial pressures, were measured. Here, we report results obtained mainly at 295 K for the films deposited in a pure O_2 environment. For impedance measurements, gold or silver paint contacts were deposited on the films' surface. The distance between contacts was varied but most of the data was obtained for a distance $L = 0.1$ mm. The current-voltage curves for these contacts were found to be Ohmic in the temperature range studied (4.2–300 K). The cross-sectional area of the films, *A*, was approximately

10^{-9} m^2. We used 100 mV excitation in our experiments. At room temperature, the films were kept inside a dark cell with controlled humidity. An UV light-emitting diode (LED) at 325 and 310 nm was used as an irradiation source.

III. RESULTS AND DISCUSSION

Structural characterization shows that the quality of our films is in line with earlier reports on sputtered IO films. The films grow in a columnar structure with a (111) preferred orientation, even in a pure Ar atmosphere [Fig. 1(a)]. The mean grain size found for the films grown in an O_2 environment is 19 ± 2 nm [Fig. 1(b)], in good agreement with our previous XRD results.[14] A TEM image, shown in Fig. 1(c), reveals that the interface region between the amorphous quartz substrate and the IO film, although not exactly flat, is abrupt. We find that the crystalline structure is preserved up to the top surface of the films. A TEM image of a boundary between two crystalline grains is shown in Fig. 1(d).

The impedance (Z) studies of the films point to at least two distinct contributions to the films' ac conductivity. This follows from the asymmetry of $-\mathrm{Im}(Z)$ vs $\mathrm{Re}(Z)$ plots, such as the ones shown in Fig. 2. The analysis of IS data is generally based on the brick layer model.[18] In this model, a polycrystalline material is formed by a three-dimensional network of cubic-shaped crystals (grains) separated by the grain boundaries. Both grains and grain boundaries have different resistivity and dielectric constant. An RC circuit is assigned to each component of the polycrystalline material and is responsible for one semicircle in the complex impedance experimental response. Grain-boundary resistivities and thicknesses obtained form the equivalent circuit are reasonable approximations provided that the grain-boundary properties are laterally homogeneous and do not vary from boundary to boundary.[19,20] Therefore, this approach is general enough to explain most experimental results.

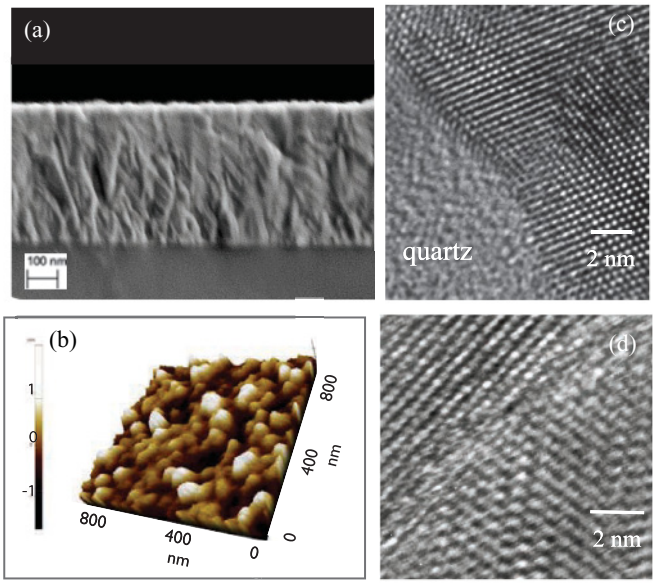

FIG. 1. (Color online) (a) SEM cross-sectional view of the film grown at $p(\mathrm{Ar}) = 1.0 \times 10^{-3}$ Torr; (b) AFM image of the surface of an In_2O_3 film deposited at $p(O_2) = 1.0 \times 10^{-3}$ Torr; and (c), (d) cross-sectional TEM images of the same IO film that are shown in (a).

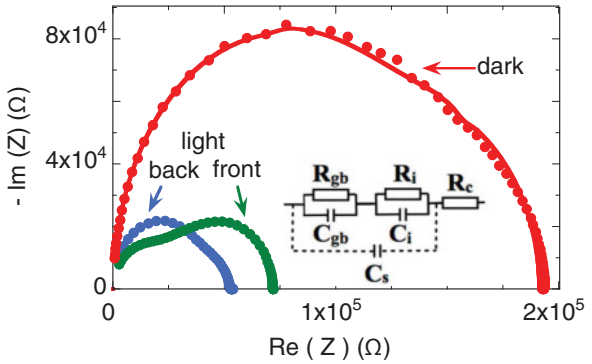

FIG. 2. (Color online) ac impedance spectra for In_2O_3 thin films grown in oxygen. Nyquist plots for an IO film in darkness and for the same film irradiated with UV light from the surface (front) and through the quartz substrate (back) are shown. The solid lines are fits to the experimental points.

We find that the impedance in darkness is the superposition of two semicircles[17] which behave differently under an UV irradiation and applied voltage bias. In terms of an equivalent circuit approximation, this corresponds to two RC circuits connected in series, as shown in Fig. 2. R_{gb},C_{gb} and R_i,C_i, are dominant in high- and low-frequency ranges, respectively. As argued below, R_{gb},C_{gb} and R_i,C_i come from grain-boundary and inversion layer conduction, respectively. We include in our circuit an additional capacitance C_s, which is brought about by the leads and sample holder, and a resistance R_c, which comes from contacts.

From numerical fittings to Z vs frequency, we obtain $C_{gb} \approx 5 \times 10^{-14}$ F. This is very close to the value we have calculated using a relative dielectric constant ϵ of 9,[1] and assuming $C_{gb} = \epsilon\epsilon_o(A/L)(L_g/w_{gb})$,[19] with $L_g/w_{gb} \approx 20$. Here, L_g is the linear grain size, and w_{gb} is the grain-boundary width. Additional support for the importance of the grain boundaries (GB) in the high-frequency region comes from UV irradiation and dc biasing experiments. In darkness, the values of C_{gb} and R_{gb} do not vary with bias voltage. Upon illumination, C_{gb} becomes a bit larger but remains independent, as R_{gb} does, of the bias voltage. Irradiation affects mainly the inversion channels whose contribution to the transport dominates in the low-frequency region. The inversion channels and the barriers at grain boundaries are connected in series. R_{gb} ($\sim 10^6$ Ω) is significantly higher than R_i and, therefore, controls the temperature variation of the dc resistivity. Figure 3 shows how the resistivity of the films grown in O_2 environment varies with temperature. We find ~0.12 eV for the conductivity activation energy in the temperature range 200–300 K. This activation value agrees well with the value for threshold voltage per boundary we obtain from IS data in a parallel geometry (the film is placed between two Ohmic electrodes). We measured impedance curves for this geometry under dc bias up to 10 V at increments of 0.2 V. Up to 2 V, little change in arcs was observed, but beyond 2 V, the arcs began to shrink in size. Such behavior supports our contention that the high-frequency arcs can be attributed to grain boundaries. The threshold voltage per boundary, calculated by dividing the overall threshold

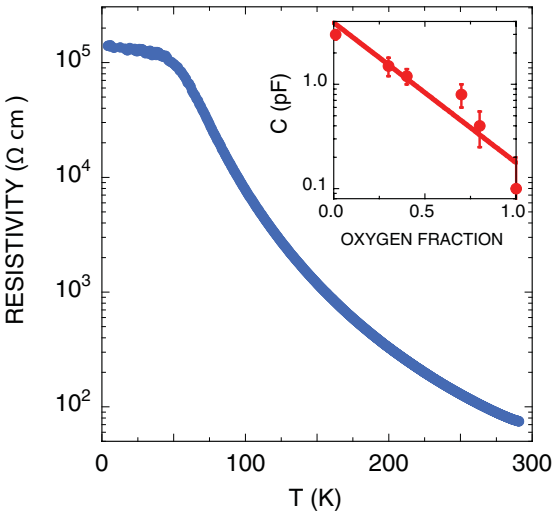

FIG. 3. (Color online) Temperature variation of the resistivity of a In_2O_3 film deposited at $p(O_2) = 1.0 \times 10^{-3}$ Torr. The inset shows the grain-boundary capacitance vs oxygen fraction in the O_2/Ar deposition gas.

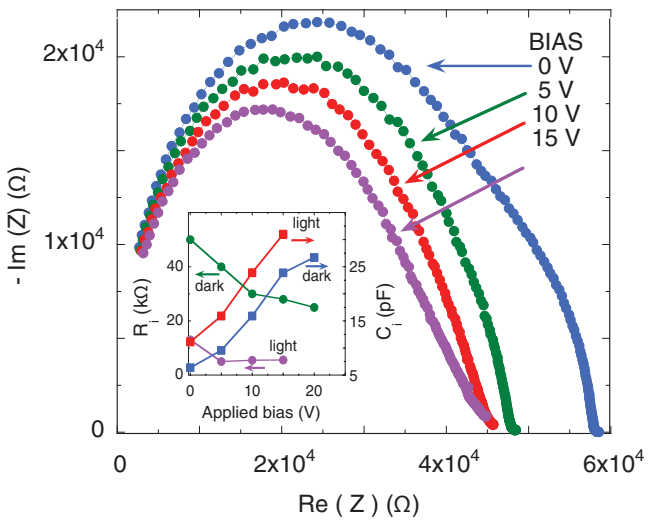

FIG. 4. (Color online) Bias-dependent Nyquist plots for an IO sample irradiated through the quartz substrate. The bias voltage variation of fitting paramaters R_i and C_i in darkness and under irradiation is shown in the inset.

voltage (2 V) by the number of grain boundaries (sample thickness/average grain size) is approximately 0.2 V, in good agreement with thermal activation energy.

In addition, we find that for films grown under various environments, C_{gb} varies systematically with the oxygen partial pressure (see inset of Fig. 3). As the oxygen partial pressure increases during the growth process, more oxygen atoms are adsorbed between grains in the films. This is brought about by the unique crystal-defect structure of bixbyite-based materials. The bixbyite structure of In_2O_3 is derived from the fluorite structure, with one-fourth of the oxygen atoms removed. These so-called "structural vacancies" are actually empty interstitial positions which favor easy incorporation of oxygen.[21] More interstitial oxygen gives rise to larger density of electronic interface states. The GB capacitance C_{gb} is inversely proportional to the square root of the GB potential barrier which, in turn, depends quadratically on the electric charge at the grain boundary and, therefore, on the density of the interface states. Consequently, a large change of C_{gb} with oxygen partial pressure is expected. All these findings support our claim that high-frequency impedance can be attributed to grain boundaries. Transport through the grains' interior, which might be expected to appear at high frequencies, does not do so.

Let us now discuss the impedance at low frequencies. Numerical fittings yield C_i values which are approximately three orders of magnitude higher than the ones found for grain boundaries. Both C_i and R_i values are significantly affected by the bias voltage and UV irradiation, as shown in the inset of Fig. 4. In addition, if the films are illuminated through a quartz substrate instead of from the surface, the form of the Nyquist plots varies, as displayed in Fig. 2. All of this points to the important role of acceptor states at the grain boundaries and at the film surface, which most likely are brought about by intergrain or surface oxygen atoms. These acceptor states capture electrons from the grains' n-type interior and, consequently, p-type inversion layers form at the grain boundaries. Such model was proposed and successfully applied to explain photoelectrical properties of thin polycrystalline PbTe films.[22,23] The capacitance of conducting inversion layers depends on the width of the space-charge region and the built-in potential. Upon illumination, the free-carrier concentration in the grains' bulk increases. Free-carrier diffusion to the grain boundaries brings about various effects. The acceptor states capture more electrons and the current of mobile photoholes in the inversion layers increases. Therefore, the resistance R_i decreases and capacitance C_i increases as the effective width of the space charge becomes smaller. Applying a voltage across the film reduces band bending in the conducting channels and, consequently, has a similar effect on R_i and C_i. In the limit of very low frequency, our dc measurements of Hall effect and thermopower under illumination unequivocally show that the mobile carriers in the films are positive and that increase of the conductivity comes mainly from increase in hole concentration. The results of the Hall-effect measurements are summarized in Table I.

The model which we put forward is schematically drawn in Fig. 5. We tentatively relate the acceptor states to intergrain or surface oxygen atoms. The frequency variation of the ratio Z_D/Z_L (dark to irradiated film's impedance) for the real and imaginary part shows maxima arising from the superposition of two different conductivity mechanisms (Fig. 6). The effect of illumination is much larger for the back configuration ($Z_D/Z_{L,f}$). No significant difference between front and back

TABLE I. Transport parameters obtained for In_2O_3 films from Hall-effect measurements at darkness and under UV steady illumination.

	Dark		UV light	
$\frac{p(O_2)}{p(O_2)+p(Ar)}$	p (cm^{-3})	σ (Ω cm)$^{-1}$	p (cm^{-3})	σ (Ω cm)$^{-1}$
0.7	2.0×10^{17}	0.017	7.9×10^{17}	0.24
1	1.2×10^{17}	0.013	2.0×10^{18}	0.60

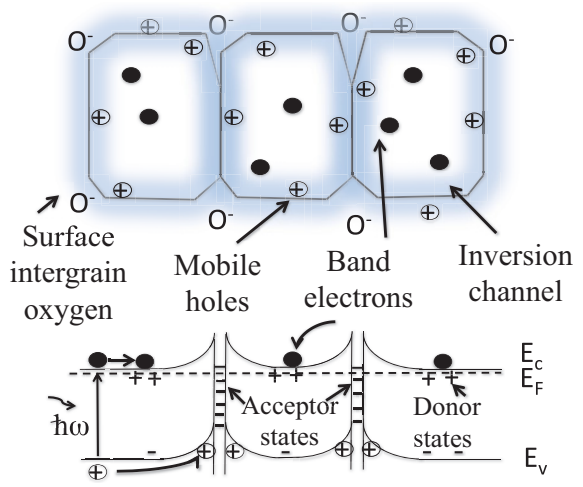

FIG. 5. (Color online) Schematic picture of grains and their boundaries. Oxygen atoms on the surface of n-type grains act as acceptors and capture electrons from the bulk of grains. A p-type inversion layer (shaded area) is formed at the grain boundaries. Surface oxygen atoms also give rise to a potential barrier for electrons as illustrated in the bottom. Therefore, the photoexcited free carriers are spatially separated and their recombination rate is low.

illuminations is observed for Z_D/Z_L at high frequencies where the grain boundaries dominate. To better define the role of the film surface, we measured the photocurrent under front and back illumination in a dry nitrogen environment and in an oxygen environment. Both rise and decay photocurrent curves follow stretched exponential time relaxations. Some important relations can be established from the comparison of saturation (steady-state) values of the photocurrent under these

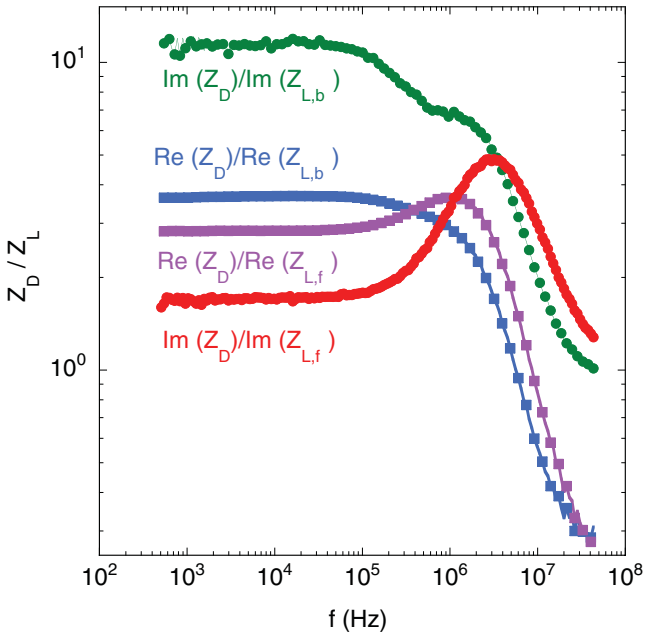

FIG. 6. (Color online) Frequency variation of the ratio Z_D/Z_L (dark to irradiated film's impedance) under front ($Z_D/Z_{L,f}$) and back ($Z_D/Z_{L,b}$) irradiation for a IO film. The solid lines are to guide the eye.

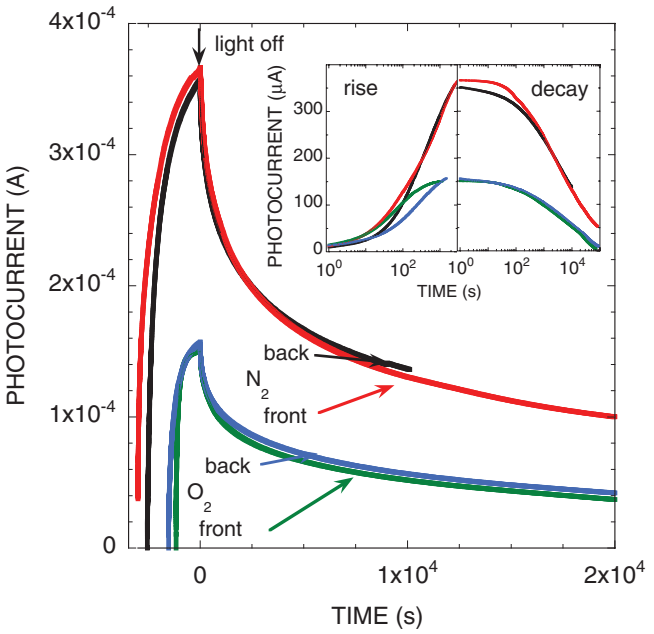

FIG. 7. (Color online) Effect of the environment (dry nitrogen and oxygen) and of experimental configuration (front and back irradiation) on the conductivity change observed upon illumination of an In_2O_3 film with a 100 mW/cm^2 UV LED at 310 nm. Inset shows the same data on the semilogarithmic scale.

conditions. For long times of illumination, the photocurrent of the sample, when surrounded by oxygen flow at one atmosphere, is actually considerably less than half of the photocurrent when the sample is surrounded by dry nitrogen. Inspection of Fig. 7 shows that surface effects are negligible under illumination with UV light in a nitrogen environment but should be accounted for in an oxygen environment. Therefore, we measure variations in the bulk conductivity (no surface effects) in the former case. For an oxygen environment, UV light additionally affects a thin surface layer with a much lower conductivity than the bulk conductivity. These two contributions to the total conductivity are additive. We obtain a value of 0.2 $(\Omega\ \mathrm{cm})^{-1}$ and 0.01 $(\Omega\ \mathrm{cm})^{-1}$ for the bulk and surface conductivities under illumination, respectively. Our calculations yield a value of 40 nm for the surface layer thickness. These surface effects can likely be attributed to the physical adsorption of oxygen.

Additional support for our model comes from XPS depth profiling experiments on the same films. We find that the O ($1s$) peak can be deconvoluted into two or three components whose amplitudes do not change noticeably after initial sputter etching.[24] This points to oxygen ions in various valence states, in agreement with the model. Final argument in favor of p-type inversion layers is brought about by photoconductivity measurements whose results are shown in Fig. 8. Ultraviolet illumination of the films leads to a sharp increase in the conductivity, followed by a very slow relaxation, on a time scale of many hours, as reported previously for n-type IO.[25] The relaxation rate of the persistent conducting state depends strongly on temperature. Cooling a film to 200 K almost completely suppresses the relaxation. We have found that the change in resistance upon illumination at 295 K arises

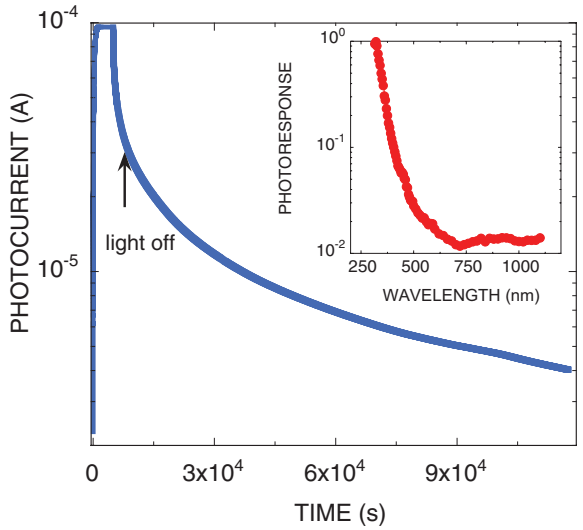

FIG. 8. (Color online) Sharp conductivity change observed upon illumination of an In_2O_3 film with a 100 mW/cm^2 UV LED at 310 nm. Normalized spectral response of photocurrent for the same film is displayed in the inset.

predominantly from an increase in the number of carriers which, from Hall-effect and Seebeck measurements, are p type. The very slow relaxation of photoinduced conductivity follows the stretched-exponential form. The stretched-exponential decay has been observed in a wide class of disordered materials, particularly in glassy materials. Several mechanisms leading to nonexponential relaxation have been proposed. One is spatial separation of excited photocarriers.[26] Our model predicts such behavior. Absorption of UV light creates hole-electron pairs as the region of greatest sensitivity is in the vicinity of the fundamental absorption edge. The hole, if sufficiently close, is attracted to the charged oxygen and increases the inversion channel conductivity. On the other hand, the electron of the hole-electron pair remains in the conduction band and does not contribute to the current because of intergrain potential barriers. The photoexcited free electrons and holes are spatially separated and, therefore, their lifetime is significantly larger than the lifetime of bulk carriers. The photocurrent decay times we have measured in very thin films (50 nm) are larger than in a thick film ($\approx$200 nm). This is consistent with charge separation, since the presence of interfaces between grains distorts energy bands in thin films more than they do in thick ones.

In sum, to explain the results obtained from ac impedance measurements for polycrystalline IO thin films, grown under O_2-rich conditions, we propose that dc conduction takes place in p-type inversion channels on the surface of crystalline grains while the grains' interior remains n type. Such mechanism might be important in other polycrystalline thin films which have a large number of oxidizing defects at grain boundaries. Being able to tune the type of dc conduction in thin films, through control of their microstructure, might open up a range of interesting applications.

ACKNOWLEDGMENTS

We thank Carmen Cosculluela for her valuable help in growing films. We acknowledge support from Grant No. MAT2008/03074, from the Ministerio de Ciencia e Innovación of Spain. Additional support from Diputación General de Aragón (DGA-CAMRADS) is also acknowledged.

*jolanta@unizar.es

[1] I. Hamberg and C. G. Granqvist, J. Appl. Phys. **60**, R123 (1986).
[2] B. G. Lewis and D. C. Paine, MRS Bull. **25**, 22 (2000).
[3] C. G. Granqvist and A. Hultåker, Thin Solid Films **411**, 1 (2002).
[4] E. Fortunato, D. Ginley, H. Hosono, and D. C. Paine, MRS Bull. **32**, 242 (2007).
[5] T. Minami, Semicond. Sci. Technol. **20**, 35 (2005).
[6] H. Kawazoe, M. Yasukawa, H. Hyodo, M. Kurita, H. Yanagi, and H. Hosono, Nature (London) **389**, 939 (1997).
[7] S. Sheng, G. Fang, C. Li, S. Xu, and X. Zhao, Phys. Status Solidi A **203**, 1891 (2006).
[8] L. Castañeda, Mater. Sci. Appl. **2**, 1233 (2011).
[9] A. Bourlange, D. J. Payne, R. G. Egdell, J. S. Foord, P. P. Edwards, M. O. Jones, A. Schertel, P. J. Dobson, and J. L. Hutchison, Appl. Phys. Lett. **92**, 092117 (2008).
[10] T. Tomita, K. Yamashita, Y. Hayafuji, and H. Adachi, Appl. Phys. Lett. **87**, 051911 (2005).
[11] S. Limpijumnong, P. Reunchan, A. Janotti, and C. G. Van de Walle, Phys. Rev. B **80**, 193202 (2009).
[12] P. D. C. King, R. L. Lichti, Y. G. Celebi, J. M. Gil, R. C. Vilao, H. V. Alberto, J. Piroto Duarte, D. J. Payne, R. G. Egdell, I. McKenzie, C. F. McConville, S. F. J. Cox, and T. D. Veal, Phys. Rev. B **80**, 081201(R) (2009).
[13] S. Lany and A. Zunger, Phys. Rev. Lett. **98**, 045501 (2007).
[14] J. Stankiewicz, F. Villuendas, and R. Alcalá, Appl. Phys. Lett. **96**, 192108 (2010).
[15] P. Reunchan, X. Zhou, S. Limpijumnong, A. Janotti, and C. G. Van de Walle, Curr. Appl. Phys. **11**, S296 (2011).
[16] P. Ágoston, P. Erhart, A. Klein, and K. Albe, J. Phys.: Condens. Matter **21**, 455801 (2009).
[17] J. R. Macdonald, *Impedance Spectroscopy Emphasizing Solid Materials and Systems* (Wiley, New York, 1987).
[18] T. Van Dijk and A. J. Burgraaf, Phys. Status Solidi A **63**, 229 (1981); M. J. Verkerk, B. J. Middelhuis, and A. J. Burgraaf, Solid State Ionics **6**, 159 (1982).
[19] J. Fleig, Solid State Ionics **150**, 181 (2002).
[20] R. Bouchet, P. Knauth, and J.-M. Laugier, J. Electrochem. Soc. **150**, E348 (2003).
[21] G. B. Gonzlez, J. B. Cohen, J.-H. Hwang, and T. O. Mason, J. Appl. Phys. **89**, 2550 (2001).
[22] L. N. Neustroev and V. V. Osipov, Sov. Phys. Semicond. **20**, 34 (1986).
[23] T. Komissarova, D. Khokhlov, L. Ryabova, Z. Dashevsky, and V. Kasiyan, Phys. Rev. B **75**, 195326 (2007).
[24] M. P. Lozano *et al.* (unpublished).
[25] A. Dixit, R. P. Panguluri, C. Sudakar, P. Kharel, P. Thapa, I. Avrutsky, R. Naik, G. Lawes, and B. Nadgorny, Appl. Phys. Lett. **94**, 252105 (2009).
[26] H. J. Queisser and D. E. Theodorou, Phys. Rev. B **33**, 4027 (1986).